Hemispheric differences of Earth's magnetic field and their implications for the magnetosphere-ionosphere-thermosphere (M-I-T) coupling

X4 . 143

Matthias Förster (1,2) and Stein Haaland (1,3)

(1) Max-Planck-Institut for Solar System Research, 37077 Göttingen, Germany (mfo@gfz-potsdam.de)
(2) GFZ German Research Centre for Geosciences, 14473 Potsdam, Germany
(3) Birkeland Center of Space Science, University of Bergen, Bergen, Norway

EGU 2018-6288 (session ST2.10 / PS 4.8)

Abstract

Disturbances in the solar wind and interplanetary magnetic field (IMF) affect the Earth's high-latitude thermosphere and ionosphere via coupling with the magnetosphere. Recent observations have shown that the upper thermospheric and ionospheric response to solar wind/IMF dependent drivers of the M-I-T system can be very dissimilar in the Northern (NH) and Southern Hemisphere (SH). Statistical studies of both ground- and satellite-based observations show hemispheric differences in the average high-latitude electric field patterns, associated with magnetospheric convection, as well as hemispheric differences in ion drift and neutral wind circulation patterns. The cross-polar neutral wind and ion drift velocities are generally larger in the NH than the SH, and the hemispheric difference shows a semi-diurnal variation. The vorticity of the upper thermospheric horizontal wind is also larger in the NH than in the SH, with larger differences for higher solar activity. In contrast, the spatial variance of the neutral wind is considerably larger in the SH polar region. These hemispheric differences can be explained at least to some extent by asymmetries in the Earth's magnetic field, both in magnetic flux density and in the offset between the geographic and invariant magnetic poles.

Cluster Electron Drift Instrument (EDI) measurements

The Electron Drift Instrument (EDI) measures the drift of a weak beam of test electrons that, when emitted in certain directions, return to the spacecraft after one gyration. This drift is related to the electric field and the gradient in the magnetic field.
Subject to certain assumptions (equipotentiality along field lines, quasi-static conditions) the average magnetospheric electric potential distribution for various IMF & solar wind conditions have been derived and mapped down to the high-latitude ionosphere of both NH & SH (Fig.1).

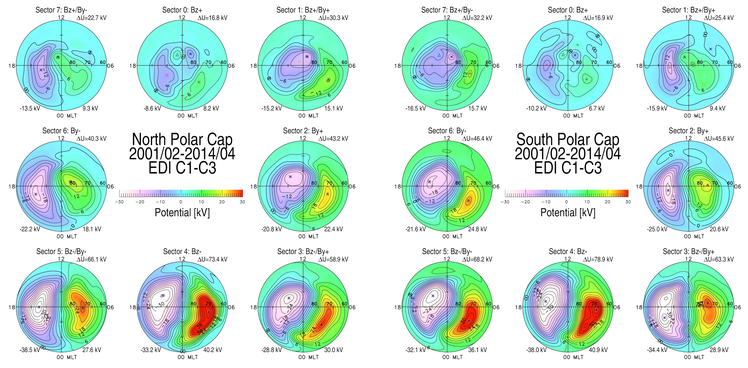

Fig. 1: Ionospheric convection patterns in the NH based on Cluster EDI observations of more than a solar cycle [see Förster & Haaland, 2015]. The data are sorted with respect to 8 different orientations of the IMF. Potential values are color-coded according to the color bar in the middle. Contour lines are drawn for every 3 kV. The minimum and maximum potential for the main cells of each IMF direction is indicated at the bottom, and the total difference (cross polar cap potential, CPCP) is given in the upper right of each individual panel.

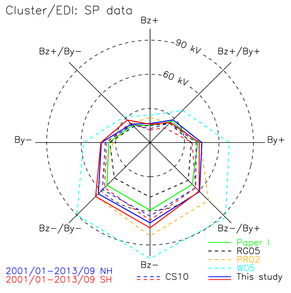

Fig. 2a: Comparison of cross polar potentials for various models for 8 IMF orientations: Blue and red lines indicate results from NH and SH, respectively (see Fig. 1). The green line indicates values from our previous EDI study (Haaland et al., 2007). The dashed black, orange, cyan, and blue/red lines are potentials reported by Ruohoniemi and Greenwald [2005], Papitashvili and Rich [2002], Weimer [2005], and Cousins and Shepherd [2010], respectively.

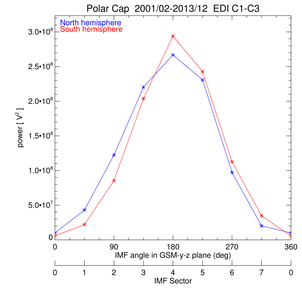

Fig. 2b: Total power of the electric field spherical harmonics potential series (in [V²]) versus the IMF angle orientation (or IMF sector numbers) for both the NH (blue) and the SH (red). The total power maximizes for southward IMF (sector 4). Interestingly, the power distributions reveal a small shift relative to each other with respect to the IMF orientation.

Geomagnetic Field Asymmetries at Ionospheric Altitude

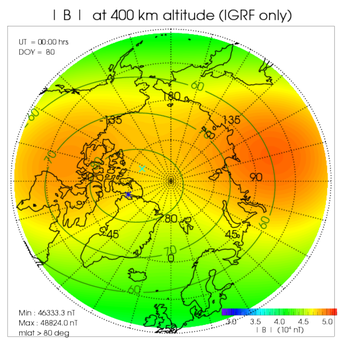

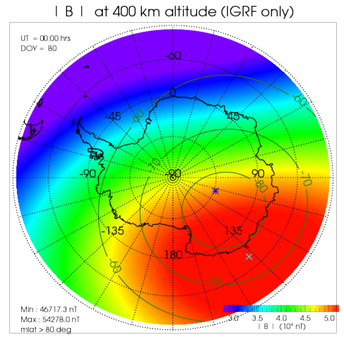

Fig. 3: Color coded maps of magnetic field strength at 400 km height for NH and SH in circular geographic coordinates around the poles with the color scale on the bottom right. The outer borders are at 50° geographic latitude; the longitudes are labeled near the 70° parallel. The magnetic field in the NH is fairly homogeneous over large regions of the polar cap with magnetic field values ranging from around 40 μT to 50 μT. The magnetic field in the SH is characterized by larger gradients and field values ranging from 24 μT to 54 μT. The dipole axis orientation (geomagnetic poles) are indicated with dark-blue asterisks and the magnetic poles (dip pole positions) with light-blue crosses. The green contour lines show geomagnetic parallels of altitude-adjusted corrected geomagnetic coordinates (AACGM).

Numerical simulations with the CMIT model have recently demonstrated that these differences can be explained at least to some extent by asymmetries in the Earth's magnetic field, both in magnetic flux density and in the offset between the geographic and invariant magnetic poles in the two hemispheres [Förster & Cnossen, 2013]. The effects of this magnetic field asymmetry on the high-latitude thermosphere and ionosphere have to be investigated more systematically. In particular, the dependence on season, IMF conditions, and solar activity level were studied by Cnossen & Förster, 2016, using CHAMP observations (see Fig. 4) and further numerical simulations. The hemispheric asymmetries constitute a certain aspect of the Earth's response to space weather as it concerns the dynamics of the high-latitude plasma convection, the neutral wind dynamics, and the mass density in the upper atmosphere. Beside increasingly sophisticated observations by ground-based networks and satellite missions, global numerical simulations based on first-principle models are an indispensable research tool.

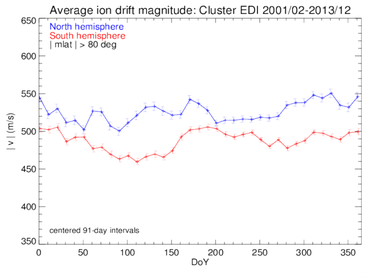

Fig. 4: 91 day running averages of the mean ion drift speed in thepolar cap (>80° magnetic latitude) for the NH (blue) and SH (red) based on EDI Cluster data from (top) February 2001 to December 2013. Error bars represent the 95% confidence intervals on the means (see Förster & Cnossen, 2016).

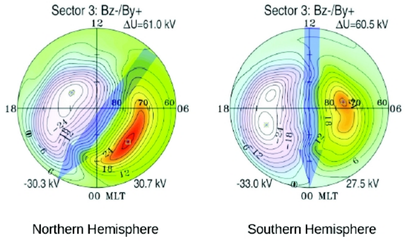

Fig. 5: Dependence of the average cross-polar (> 80 deg magnetic latitude) neutral wind magnitude at 400 km and its direction on the IMF orientation (sector number 4 = southward IMF, 0 = purely northward IMF). The dashed lines show the variance of the average values.

Table 1. Cross-polar cap potential (CPCP) drop between the main cells of the statistical plasma drift patterns obtained from mapped spin-resolution EDI Cluster measurements (PP data) for 8 separate IMF sectors. The first two data columns comprise the whole interval of EDI measurements obtained up to now (2001/02-2013/12) for both the NH and SH; the middle pair of columns are from the initial period of high solar activity (2001–2003), and the final pair of columns shows the low solar activity conditions (2005–2010) [from Förster & Haaland, 2015].

IMF	Cross-polar cap potentials, CPCP [kV]					
	2001–2013		2001–2003		2005–2010	
# sector / direction	all data		high solar activity		low solar activity	
	NH	SH	NH	SH	NH	SH
0 B_z+	19.0	16.0	17.4	21.1	21.1	15.0
1 B_z+/B_y+	27.0	24.4	35.7	44.9	27.6	23.3
2 B_y+	43.8	42.4	54.3	51.3	42.5	38.6
3 B_z-/B_y+	57.7	57.1	70.7	72.2	53.9	53.1
4 B_z-	65.0	70.2	77.6	85.5	60.9	61.9
5 B_z-/B_y-	61.9	65.0	65.2	75.8	58.0	54.8
6 B_y-	42.6	42.1	47.8	49.7	37.6	39.5
7 B_z+/B_y-	22.7	26.7	27.2	31.3	24.4	24.1

CHAMP Accelerometer Neutral Wind Measurements

The Challenging Minisatellite Payload (CHAMP), which is managed by the GFZ German Centre of Geosciences in Potsdam, was launched in summer 2000 into a near-circular near-polar orbit at ~460 km with an inclination of ~87.3°. During the years 2002 & 2003, its orbital altitude had decayed to about 400 km. One key scientific instrument on board CHAMP is a triaxial accelerometer. From the air drag observations, thermospheric mass density and cross-track neutral wind can be obtained using the methodology described by Doornbos et al., 2010.

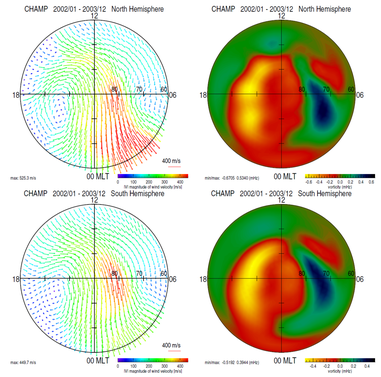

Fig. 6: Average thermospheric wind pattern at ~400 km altitude over the polar region of the NH and the SH obtained from CHAMP accelerometer measurements over the whole years of 2002-2003. The MLT versus magnetic latitude dials have an outer boundary of 60°; the projection of the SH is such as looking from North through a transparent Earth. The color scales of the color coded neutral wind vectors (left column) and neutral wind vorticity values (right column) are given at the bottom right of each individual panel (please note the different scale lengths). The neutral wind patterns are additionally scaled by the length of the wind vector arrows.
The neutral wind vorticity patterns (radial component) on the right hand side are derived from the average neutral wind pattern on the left side. Negative vorticity values (red to yellow) indicate a clockwise, positive (green to blue) a counterclockwise circulation. The minimum and maximum vorticity values are indicated at the bottom left side of the right panels (Förster et al, 2008, 2017).

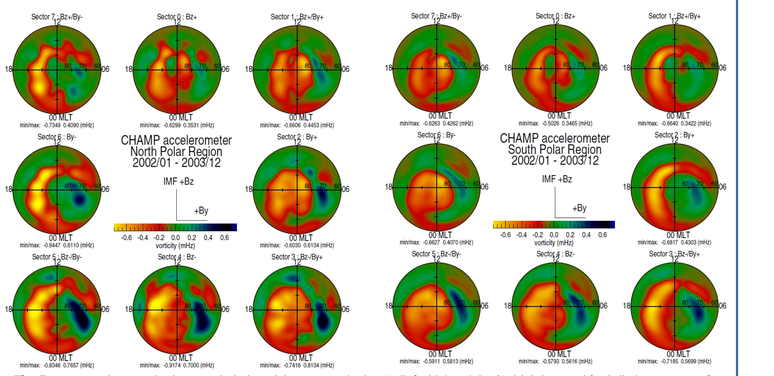

Fig. 7: Average thermospheric neutral wind vorticity patterns in the NH (left side) and the SH (right), sorted for 8 distinct sectors of IMF orientation as it was done for the ionospheric E × B drift pattern in Figure 1. Each sector comprise hence 45 deg of IMF clock angle range centered around the direction indicated on top of each panel.

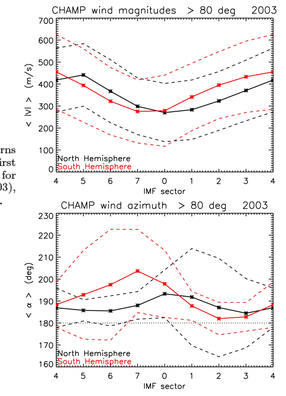

References:

Cnossen, I. and M. Förster (2016), North-South asymmetries in the polar thermosphere-ionosphere system: Solar cycle and seasonal influences, J. Geophys. Res., 121(1), 612-627, doi:10.1002/2015JA021750..

Cousins, E. D. P., and S. G. Shepherd (2010), A dynamical model of high-latitude convection derived from SuperDARN plasma drift measurements, J. Geophys. Res., 115, A12329, doi:10.1029/2010JA016017.

Doornbos, E., J. van den IJssel, H. Lühr, M. Förster, and G. Koppenwallner (2010), Neutral density and crosswind determination from arbitrarily oriented multi-axis accelerometers on satellites, J. Spacecraft and Rockets, 47(4), 580–589, doi:10.2514/1.48114.

Förster, M., G. Paschmann, S. E. Haaland, J. M. Quinn, R. B. Torbert, C. E. McIlwain, H. Vaith, P. A. Puhl-Quinn, and C. A. Kletzing (2007), High-latitude plasma convection from Cluster EDI: Variances and solar wind correlations, Ann. Geophys., 25(7), 1691-1707.

Förster, M., S. Rentz, W. Köhler, H. Liu, and S. E. Haaland (2008), IMF dependence of high-latitude thermospheric wind pattern derived from CHAMP cross-track measurements, Ann.Geophys., 26(6), 1581-1595.

Förster, M., and I. Cnossen (2013), Upper atmosphere differences between northern and southern high latitudes: The role of magnetic field asymmetry, J. Geophys. Res., 118(9), 5951-5966, doi:10.1002/jgra.50554.

Förster, M., and S. Haaland (2015), Interhemispheric differences in ionospheric convection: Cluster EDI observations revisited, J. Geophys. Res., 120(7), 5805-5823, doi: 10.1002/2014JA020774.

Förster, M., E. Doornbos, and S. Haaland (2017), The role of the upper atmosphere for dawn-dusk differences in the coupled magnetosphere-ionosphere-thermosphere system, in: AGU Geophysical Monograph No. 230 on 'Dawn-Dusk Asymmetries in Planetary Plasma Environments', 125-142.

Haaland, S. E., G. Paschmann, M. Förster, J. M. Quinn, R. B.Torbert, C. E. McIlwain, H. Vaith, P. A. Puhl-Quinn, and C. A. Kletzing (2007), High-latitude plasma convection from Cluster EDI measurements: Method and IMF-dependence, Ann. Geophys., 25(1), 239-253.

Papitashvili, V. O., and F. J. Rich (2002), High-latitude ionospheric convection models derived from Defense Meteorological Satellite Program ion drift observations and parameterized by the interplanetary magnetic field strength and direction, J. Geophys. Res., 107(A8), 1198, doi:10.1029/2001JA000264.

Ruohoniemi, J. M., and R. A. Greenwald (2005), Dependencies of high-latitude plasma convection: Consideration of interplanetary magnetic field, seasonal, and universal time factors instatistical patterns, J. Geophys. Res., 110(A9), A09204, doi: 10.1029/2004JA010815.

Weimer, D. R. (2005), Improved ionospheric electrodynamic models and application to calculating Joule heating rates, J. Geophys. Res., 110(A5), A05306, doi:10.1029/2004JA010884.